Journal of Molecular Graphics and Modelling 43 (2013) 58–65

Contents lists available at SciVerse ScienceDirect

Journal of Molecular Graphics and Modelling

journal homepage: www.elsevier.com/locate/JMGM

A theoretical study on mechanism of the anticancer drug camptothecin's E-ring-opening

Hui-Yuan Zou, Dong-Xia Zhao, Zhong-Zhi Yang*

Chemistry and Chemical Engineering Faculty, Liaoning Normal University, Dalian 116029, China

ARTICLE INFO

Article history:
Accepted 23 March 2013
Available online 17 April 2013

Keywords:
Camptothecin
Hydrolysis
E-ring-opening
DFT
IEF-PCM
Anticancer

ABSTRACT

A reaction mechanism of the anticancer agent camptothecin (CPT)'s E-ring-opening has been studied by DFT method and IEF-PCM solvation model. Our results indicate that under the physiological PH, CPT's E-ring-opening is a spontaneous process, and it conforms to the addition coupled elimination reaction pathway with a proton translocation. The obtained activation free energies in the explicit water model are in agreement with the available experimental values. More than ten reactions have been studied to provide exhaustive analyses of the relationship between structure and reactivity. On the whole, our results accord with the experimental findings and the mechanism we proposed is reasonable.

1. Introduction

Camptothecin (CPT) is a plant alkaloid in the Chinese tree *Camptotheca acuminate*. It was first discovered and identified by Monroe Wall and co-workers in 1966 [1,2]. The basic compound CPT ($C_{20}H_{16}N_2O_4$), see Fig. 1, has a planar pentacyclic ring structure with a pyrrolo[3-4-β]quinoline moiety (rings A, B, and C), a conjugated pyridone group (ring D), and one α-hydroxy lactone ring (the E-ring) [3]. The pharmacological investigations into CPT had been suspended on one occasion for its poor solubility in water and most organic solvents (ex DMSO). Then CPT's E-ring was opened and modified with sodium carboxylate, which obviously improved CPT's water-solubility, but also reduced its pharmacological activity [4]. Until 1985, much attention had been paid to CPT again, for its particular medication function was posted [5,6]. CPT and its derivatives are the prototypical class of topoisomerase I (Top1) inhibitors with significant activities against a broad range of human tumors. They play a key role in effectively preventing the Top1-DNA cleavage complex (Top1cc) from dissociation by intercalating reversibly to the DNA cleavage site produced by Top1, resulting in double-stranded DNA damage and apoptosis eventually [7–9].

Today, CPT is becoming one of the most promising antimetastatic agents that have successfully completed phase I clinical trials [10]. However, one of the main limitations of CPT is its spontaneous and rapid inactivation (within minutes) by E-ring-opening, i.e., from an active lactone form to an inactive hydrolyzed carboxylate form (Fig. 2) [11,12]. Although this reaction is potentially reversible, its equilibrium favors the carboxylate form at the physiological conditions [10,13]. Investigations on several E-ring modified CPT analogs concluded that the biologically active-α-hydroxyl lactone moiety is indispensable for antitumor activity [14–18]. Chemical modifications of the lactone ring, such as transformation into a lactam ring, removal of the carbonyl oxygen, or substitution of the 20-hydroxyl group by hydrogen, inactivate the molecule. Thus an intact lactone form is believed to be the pharmacological active one [19].

Some structural and biochemical studies of CPT by electronic, fluorescence, EPR and NMR spectroscopy have been previously carried out [16,20–23]. Experimental and theoretical analyses indicate that the stabilization of CPT and its analogs in solution strongly depend on PH, concentration and solvent surrounding [24,25]. The processes of CPT's E-ring-opening have been recently studied by experimental tests as well. Afzal Shaha et al. have proposed the electrochemical reduction mechanism of CPT by voltammetry measurements [19]. Kunadharaju and Savva have tested the thermodynamic parameters of 10-hydroxy-CPT's lactone ring hydrolysis at the physiological PH by using derivative spectrophotometric technique [26].

However, to the best of our knowledge, a comprehensive theoretical study on the mechanism of CPT's inactivation reaction has not been reported yet. Investigations into the E-ring-opening process by computational tool would provide complements to experimental data, and further promote the pharmacological activity of drugs like CPT. In the present work, the mechanism of CPT's E-ring-opening was studied by applying the density functional theory (DFT) and the isoelectric focusing polarized continuum model

* Corresponding author. Tel.: +86 411 82159607; fax: +86 411 82158977.
E-mail address: zzyang@lnnu.edu.cn (Z.-Z. Yang).

1093-3263/$ – see front matter © 2013 Elsevier Inc. All rights reserved.
http://dx.doi.org/10.1016/j.jmgm.2013.03.004

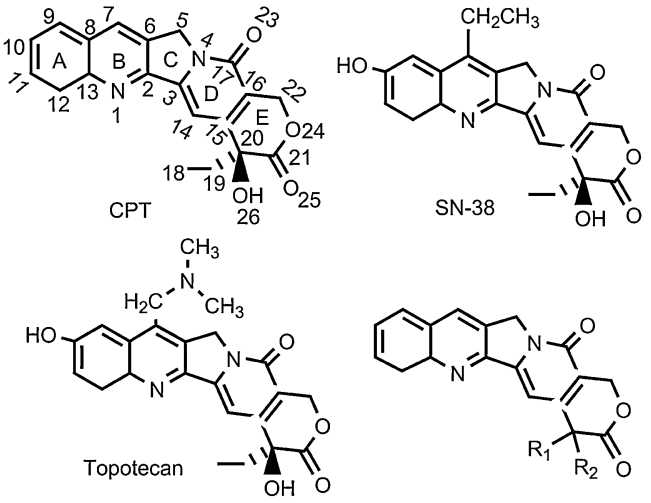

Fig. 1. Molecular structures of CPT (with its corresponding numbering), SN-38, Topotecan, and analogs of CPT with different substituents R_1 and R_2 respectively.

(IEF-PCM) for the first time. Some spectroscopic analyses of CPT and its derivatives demonstrated that CPT and its analogs trend to aggregate in solution, especially in dimer formation, and the E-ring-opening process occurs at neutral PH [24,25,27]. The main purpose of this paper is to reveal the E-ring-opening mechanism of CPT, therefore, considering of computational cost our calculations were performed under the physiological PH with a concentration low enough ($<10^{-5}$ M), which CPT and its analogs were reported in monomeric forms [24]. In addition, although various tautomers of CPT's derivative have been proved to coexist in aqueous solution, the presence or absence of E-ring does not affect at all the structure of the remaining part of the molecule [25,27]. The energies we concerned, the activation and reaction free energies, are relative values between intermediates and transition states, and reactants and products, respectively. The obtained results would get little influence if no obvious structural changes of other rings happen. Thus, searching for the most stable forms of the reactants does not been included in this work.

In this work, the most possible reaction path for CPT's E-ring-opening was proposed, and the analyses of charge distribution and solvent effect were presented. Moreover, reactions with different substituents on A, B and E rings were also studied to reveal the relationship between structure and reactivity. This study may be helpful for people to understand the reaction process and would be useful in the design of novel CPT-based anticancer agents.

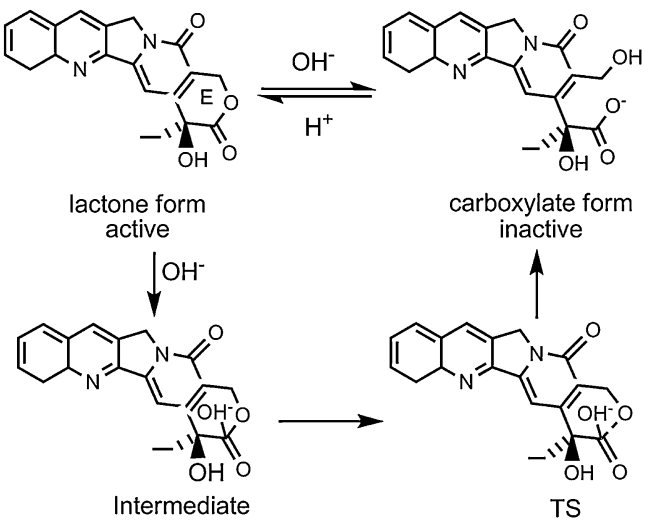

Fig. 2. The proposed E-ring-opening mechanism of CPT. From the active lactone form to its inactive carboxylate derivative includes an intermediate and a transition state.

2. Computational details

The process of CPT's E-ring-opening as shown in Fig. 2 was chosen to perform the test calculations. All the structures, including two reactants (R), an intermediate (I), a transition state (TS), and a product (P), were respectively optimized at B3LYP [28]/6−31G(d,p), B3LYP/6−311+G(d,p) and MP2 [29]/6−31G(d,p) levels by using the Gaussian 03 [30] program (Table S1, Supporting Information). We found that the MP2/6−311+G(d,p)//MP2/6−31G(d,p) method does an excellent work in the calculation of activation free energies, but requires a significant increase in computational time. Thus all the balanceable stationary points of the hydrolysis reactions like CPT were optimized at the B3LYP/6−31G(d,p) level of theory. Since the anion calculations in gas phase by DFT are dangerous (see Section 3.1.3), a nonpolar solvent carbon tetrachloride (CCl_4) in PCM formalism was employed when all the optimizations were carried out. Harmonic frequencies were calculated in vacuo based on the optimized configurations also at the B3LYP/6−31G(d,p) level to extract the thermal energy contributions at 298 K and 1 atm. All the transition states were further confirmed by intrinsic reaction coordinate (IRC) [31,32] calculations. In addition, the intermediates and the products were respectively obtained by standard structural optimizations following the corresponding IRC in both directions. Solvation free energies were estimated on the basis of the optimized geometries by using the IEF-PCM model [33–35] at the MP2/6−311+G(d,p) level with UAHF atomic radii. The dielectric constant of water ($\varepsilon = 78.39$) was employed to approximate the bulk effects of solvent. The activation free energy and the reaction free energy were respectively calculated by comparing TS with I, and P with R at the hybrid MP2/6−311+G(d,p)//B3LYP/6−31G(d,p) level of theory. For the sake of clarity, the activation free energy was labeled as ΔG_a, and the ΔG_a in gas phase and aqueous solution were labeled as ΔG_a^g and ΔG_a^a, respectively. Similarly, the reaction free energy in aqueous solution was reported as ΔG_r^a.

3. Results and discussion

3.1. E-ring-opening mechanism of CPT

3.1.1. Mechanism

Fig. 3 displays the most likely reaction path for CPT's E-ring-opening, including the separated reactants: CPT and OH^-, the intermediate, the transition state, and the product. Results suggest that the CPT's E-ring-opening reaction proceeds through an addition coupled elimination mechanism under the physiological PH. Although this is a reversible process, from the lactone form to the carboxylate form is a spontaneous direction because a negative value of the ΔG_r^a is obtained. At the physiological PH, a hydroxyl from water or alkalescent favors to attack C21 of lactone with forming a new bond, while the single bond C21—O24 is lengthened from 1.34 to 1.49 Å, resulting in forming an intermediate. Then the labile intermediate decomposes, and follows a transition state. The transition state is characterized by an imaginary frequency of 179 cm^{-1}, in which the C21—O24 bond is breaking. The distance between C21 and O43 (the atom of the entering hydroxyl) reduces from 1.47 Å in I to 1.40 Å in TS, and the C21—O24 distance increases from 1.49 to 1.98 Å. In the product, the distance between C21 and O24 is 3.23 Å, i.e., the E-ring has been completely opened, and a proton transfers from the entering hydroxyl to O24 to form a hydrogen bond (1.56 Å) with O43. (The corresponding structures of stationary points are shown in Fig. S1, Supporting Information.)

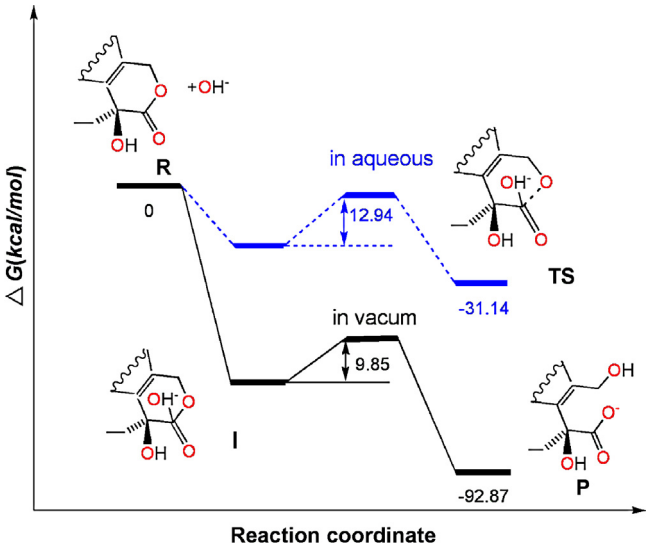

Fig. 3. Calculated reaction profiles of the CPT's E-ring-opening, solid lines: free energies in vacuo, dashed lines: free energies in aqueous phase. (All the structures along the process are in Fig. S1. Supporting Information.).

The calculated ΔG_a^g and ΔG_a^a of CPT's E-ring-opening are 9.85 and 12.94 kcal/mol, respectively. These indicate that the polarization effect of solvent slackens the reaction by enhancing its ΔG_a. This will be further demonstrated in Section 3.1.3. Referring to the experimental value of 10-hydroxy-CPT, 18.98 ± 0.22 kcal/mol at a temperature of 310 K, our results in aqueous solution at 298 K underestimates the ΔG_a. Except different species, there are another three possible reasons. Firstly, the two temperatures are different. However, after the test calculations we found that promoting temperature from 298 K to 310 K changes the related energies with a negligible difference. The exact energies were provided in Table S2, Supporting Information. Secondly, the reactants we selected are different from those of experiment. The reactants employed by Kunadharaju and Savva are 10-hydroxy-CPT and a water molecule [26], while we found it is difficult for such a weak nucleophile like water to attack CPT's E-ring, so that the water molecule was replaced by a hydroxyl. Finally, the method employed in structural optimization also impacts on the values of ΔG_a^a, for example, the ΔG_a^a obtained by MP2/6−311+G(d,p)//MP2/6−31G(d,p) method is 15.94 kcal/mol, which is much closer to the experimental results. The addition coupled elimination mechanism is therefore regarded as the most possible reaction path for the E-ring-opening of CPT and its analogs.

3.1.2. Analysis of charge distribution

Fig. 4 displays the charge distributions of several key atoms during the course of E-ring-opening, which were obtained by the atom-bond electronegativity equalization $\sigma\pi$ model (ABEEM$\sigma\pi$). The ABEEM$\sigma\pi$ is based on the density functional theory and electronegativity equalization principle, and it is a fast and effective method for calculating the charge distribution of various molecules [36,37], such as macromolecules, biomolecules, aqua ions, pharmic molecules and so on. Since the ABEEM charge distribution is the foundation of ABEEM$\sigma\pi$ polarizable force field (ABEEM/MM) [38], we fitted the parameters and calculated the charges of CPT in ABEEM$\sigma\pi$ model for the further dynamic simulations by ABEEM/MM. Parameters of CPT were listed in Table S3, Supporting Information. Corresponding to the structural changes during the E-ring-opening course, the remarkable changes of charge are on three atoms, the central C21 atom, the attacking O43 atom, and the leaving O24 atom. The trend in the charge changes can be clearly seen in Fig. 4. The positive charge of C21 first increases and then reduces especially after TS because of the cleavage of C21—O24 bond. The biggest positive charge of C21 is on TS, which is relevant to the leaving of O24. Compared with the isolated hydroxyl, the net charge of O43 becomes smaller since some negative charges have been transferred to CPT, which is favorable for the E-ring-opening. In addition, the charge changing features of the attacking O43 and the leaving O24 have the opposite trends. All of above indicates that charge transfers do occur in the process of E-ring-opening.

3.1.3. The solvent effect

In this section, comparisons of the solvent effect on the E-ring-opening mechanism were divided up into two groups, including four computational models. The first comparison was presented between the results in gas phase and in CCl_4 (with PCM model). In vacuo, there are two transition states (TS). The first one (TS1) corresponds to the vibration of hydroxyl between C16 and C21, and in the second TS (TS2), the bond between C21 and O24 is breaking. Both the two TSs were confirmed by IRC calculations. The corresponding product of the first step has nearly the same energy and configuration with the reactant of the second step. Thus we once deemed that the whole process showed in Fig. S2 (Supporting Information) is the reaction path that CPT followed to open its E-ring. However, when the TS1 was re-optimized in CCl_4, the entering hydroxyl is vibrating with C16 without C21. Further IRC calculations showed that the obtained reactant and product correspond to the same one, i.e., the reactant, which indicates that TS1 is not valid and should be discarded. Therefore, anion calculations in gas phase are always dangerous and should be avoided, especially by DFT method. Combing DFT with nonpolar solvent would solve this problem. As listed in Table 1, all the stationary points hold the similar features of structure in gas phase and in CCl_4. The reaction process obtained in CCl_4 proposed in Section 3.1.1 is in good agreement with the electrochemical reduction mechanism of CPT, and moreover, it also accords to the one that optimized by MP2 method, but with a lower computational cost.

The other comparison of solvent effect was carried out between explicit and implicit (the PCM) water models. On the one hand, we add one and two explicit water molecules to the hydroxyl anion as the reactants, respectively, and then the reaction mechanism was studied again in CCl_4. On the other hand, all the stationary points

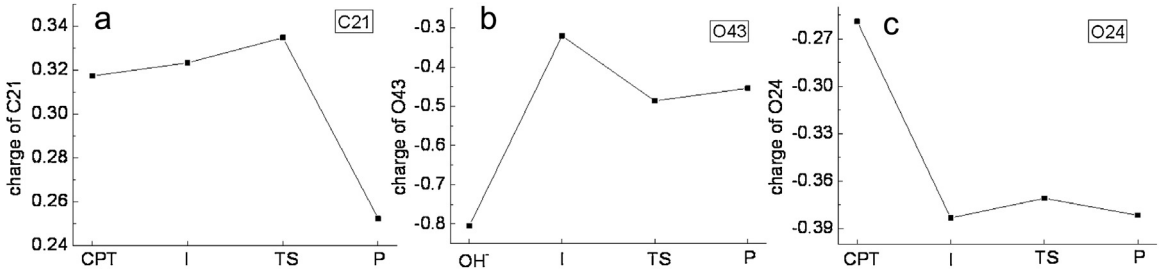

Fig. 4. The ABEEM $\sigma\pi$ charges of three important atoms, the central C21, the attacking O43 and the leaving O24, along the reaction course.

Table 1
Some bond length parameters (in Å) for all stationary points along the reaction path in the E-ring-opening reaction of CPT with different solvent models.

Solvent models	I		TS	P
	C21—O24	C21—O43	C21—O24	O24—H···O43
Non (in vacuo)	1.4956	1.4658	1.9693	1.5521
In CCl_4 (PCM)	1.4879	1.4651	1.9782	1.5634
H_2O + in CCl_4	1.4743	1.4702	2.0428	1.5966
$2H_2O$ + in CCl_4	1.4612	1.4758	2.0531	1.7529
In water (PCM)	1.4831	1.4492	2.0902	1.5906

Table 2
The computed ΔG_a and ΔG_r (in kcal/mol) of CPT with different number of explicit water molecules (n = 0,1,2), and in PCM model.

	ΔG_a^g	ΔG_a^a	ΔG_r^a
CPT + OH^- (in CCl_4)	9.85	12.94	−31.84
CPT + OH^- + H_2O	13.93	15.58	−21.96
CPT + OH^- + $2H_2O$	16.02	15.01	−12.79
CPT + OH^- + (ε = 78.39)	9.41	11.96	−31.42

along the reaction path have been re-optimized using the PCM model with aqueous dielectric constant. Some selected structural parameters and correlative energies are listed in Tables 1 and 3, respectively.

Comparing the data listed in Table 1, it can be found that both solvent models have influence on the structures of the stationary point. As the number of explicit water molecules increases, the distances between C21 and O24 shorten, while those of C21 and O43 lengthen in the intermediates. Analyzing the hydrogen bonds of the two intermediates shown in Fig. 5, we can see that the interactions between explicit water molecules and the E-ring of CPT concentrate among the 20-hydroxyl, the carbonyl oxygen and the attacking hydroxyl. When one and two water molecules participated, they interact with the entering hydroxyl by forming one and three hydrogen bonds, respectively. That is to say, in the latter case, the hydroxyl interacts with water molecules stronger than CPT with increasing the distance between C21 and O43, which leads to an effect of weakening the C21—O24 bond. On the contrary, since the absent description of hydrogen bond in PCM water model, the C21—O43 and C21—O24 bonds hold the opposite rule with explicit water model, and the obtained intermediate inclines to the TS. In TS, the bond of C21 and O24 is breaking. Similar to in intermediates, the more hydrogen bonds form, the steadier the new forming carboxyl is, the less restriction on O24 is, resulting in an easier E-ring-opening of CPT, and the distances between C21 and O24 increase. In products, the lactone ring was opened with a proton transfer from the attacking hydroxyl to O24, and forming a hydrogen bond with O43. Expect the smallest distance of this hydrogen bond in PCM water model, the lengths of others lengthen as the number of explicit water molecules increases. By this token, hydrogen bond is an indispensable factor that plays a key role in effecting the E-ring-opening process of CPT.

Similarly, solvent impacts on relative energies of E-ring-opening reaction as well. From Table 2, it can be seen that the ΔG_a^g increases as the number of participated water molecules rises. As shown in Fig. 5, no matter in which state, the hydroxyl uses its oxygen to form hydrogen bonds with the hydrogen atoms of water. This is in good agreement with the conclusions of the studies on the hydroxide ion-water clusters [39–41]. Some negative charges of O43 transfer to the hydrogen atoms of water through hydrogen bonds, so that CPT receives less negative charges from the hydroxyl, resulting in the reduction of electron density on O24. The CPT's E-ring-opening is a process of O24 leaving, since the more negative charges on O24, the easier for it to disconnect with C21, thus the reaction energy barriers increase as the hydrogen bonds formed. The ΔG_a^a of adding one and two water molecules are 15.58 and 15.01 kcal/mol, respectively. The ΔG_r^a increases when more water molecules are added, since the introducing of water increases the energies of reactant, though more hydrogen bonds are formed in the products. However, compared with the explicit water model herein, the PCM model does not improve the results, or even worse. As we discussed above, the I in this model is closer than the ones in explicit water model to

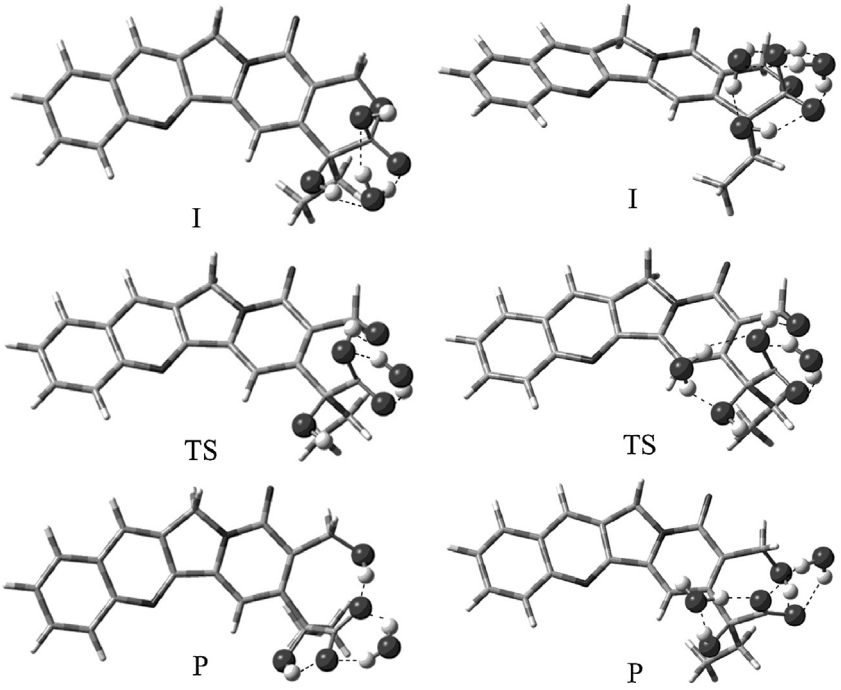

Fig. 5. Molecular structures of stationary points (I, TS, and P) along the reaction path of CPT's E-ring-opening in the one (left row) and the two (right row) explicit water model, respectively. The backbone is shown in sticks. The dashed lines indicate hydrogen bonds. For the sake of clarity, the relative atoms of hydrogen bond are displayed in ball and bond type. The black ball denotes the oxygen, and the write one is hydrogen.

TS, thus the energy barrier between TS and I reduces. In addition, further studies of adding three water molecules to the hydroxyl have also been attempted. The stable structures indicate that the third water molecule interacts with CPT and other water molecules replacing the hydroxyl, and we have not found any accurate TS yet. Although there are just two explicit water molecules, this model is closer to the real species. A higher level ab initio method or a hybrid QM/MM [42–44] method would improve the results to achieve better agreement with the experimental observations. Therefore, we proposed that the addition coupled elimination mechanism is a credible reaction path for CPT to open its E-ring.

3.2. The influence of substituents

When the special medication function of CPT was revealed, numerous hemi-synthetic derivatives were developed to achieve better water solubility and fewer side effects. With the purpose to reveal the relationship between structure and reactivity, we selected some analogs which were modified by A, B and E rings, but except C and D rings, since modifying ring C and D would descend or even disable the pharmacological activities [45].

3.2.1. E-ring modifications

The (S) stereochemistry and the hydroxyl group at position 20 are generally regarded as the pharmic active center of CPT [46]. Thus we further studied on site 20 with different substituents to investigate the influence of substituent. It should be noticed that our purpose is to investigate the relationship between structure and reactivity, so that some systems were constructed without considering the practical significance.

Fig. 6a and b shows the relative energies that R_2 was kept as hydroxyl while R_1, ethyl, was replaced with hydrogen, methyl, and isopropyl, respectively (see Fig. 1). It can be seen that as the electron-donating capability of the substituent rises, the negative charge of C20 increases because of the electronic effect. Due to the inductive effect the positive charge of C21 increases as well. Thus the bond between C21 and O24 becomes much stronger caused by the increasing electrostatic interaction, which is disadvantage for O24 to leave, so that the ΔG_a^g (the solid line) in Fig. 6a increase. However, when solvation has been taken into account, the ΔG_a^a (the dashed line) in Fig. 6a decreases as the size of the substituent increases, while the ΔG_r^a in Fig. 6b increases. The electrostatic interaction term of solvation free energy (ΔG_{sol}) may bear the main contribution of the decrease of ΔG_a^a. The difference of ΔG_{sol} between the reactant and transition state reduces with the increase of the substituent's sizes, whereas those of the ΔG_a^g increase progressively. The degrees of ΔG_{sol} reduced are greater than those of ΔG_a^g augmented, so the ΔG_a^a decrease finally. Although the ΔG_r^a increases, all the E-ring-opening reactions with different substituent groups are spontaneous processes.

On the other hand, Fig. 6c and d shows the relative free energies that ethyl (R_1) was retained while the hydroxyl of R_2 was displaced by various substituents. As shown in the solid line of Fig. 6c, the ΔG_a^g increases undulantely with the electron-donating powers of the substituent, H, CH_3, OCH_3, OH, and NH_2. Besides the electronic and inductive effects, the stability of intermediate is another key factor to decide the activation energy barriers. As shown in Fig. 7, the ΔG_a^g of different substituents, OH, NH_2, CH_3, OCH_3 and H, decrease as the distances between C21 and O24 lengthen, because the shorter the bond length is, the steadier the intermediate is. Since the intermediate of OH, who has the shortest C21—O24 bond, 1.49 Å, and an intramolecular hydrogen bond, is the most stable, the reaction of OH corresponds to the biggest ΔG_a^g, 9.85 kcal/mol. Although the difference of bond length between CN and NH_2 is small, the gap of corresponding ΔG_a is wide, because NH_2 is an electron-donating group and CN is an electron-withdrawing group. In contrast to the electron-donating groups, the ΔG_a^g of electron-withdrawing groups decrease as the electron-withdrawing capabilities of substituent rise. Because the electronic densities of C20 descend with the augment of electron-withdrawing capabilities of CN and Cl, the positive charges of C21 that generate by inductive effect diminish, resulting in the weakening electrostatic interaction between C21 and O24, so that it is easy for O24 to leave with a lower ΔG_a^g. All the reactions we studied are thermodynamic spontaneous processes.

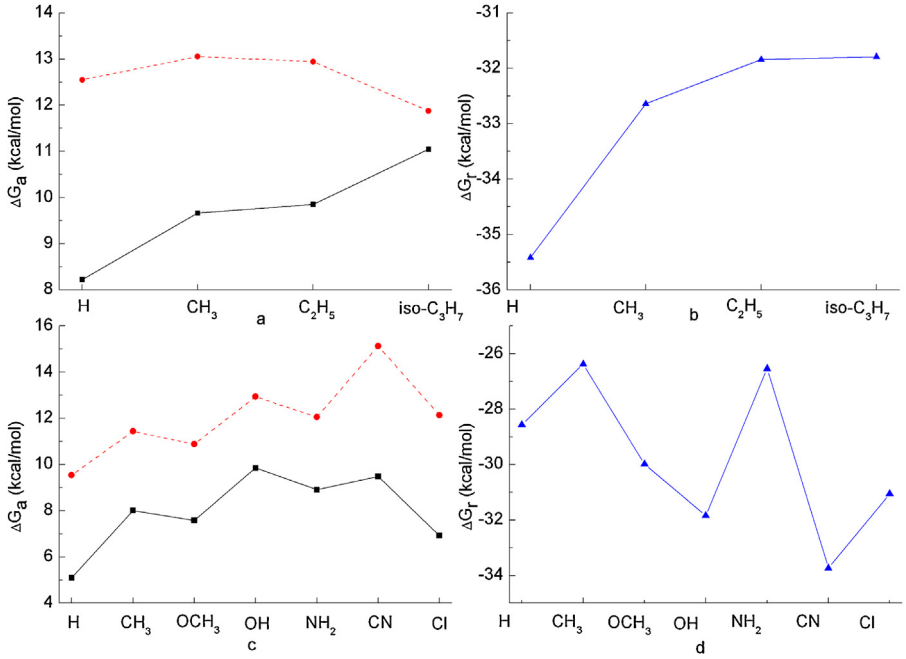

Fig. 6. Calculated activation and reaction free energies related to different substituents. The top two schemata corresponding to the relative energies of the substituents that R_2 = OH and R_1 = H, CH_3, C_2H_5, iso-C_3H_7 in turn. The schema (a) displays the ΔG_a^g (solid line) and the ΔG_a^a (dashed line) respectively, and the schema (b) displays the ΔG_r^a. The bottom schemata corresponding to the relative energies of the substituents that R_1 = C_2H_5 and R_2 = H, CH_3, OCH_3, OH, NH_2, CN, and Cl in turn. The schema (c) displays the ΔG_a^g (solid line) and the ΔG_a^a (dashed line) respectively, and the schema (d) displays the ΔG_r^a.

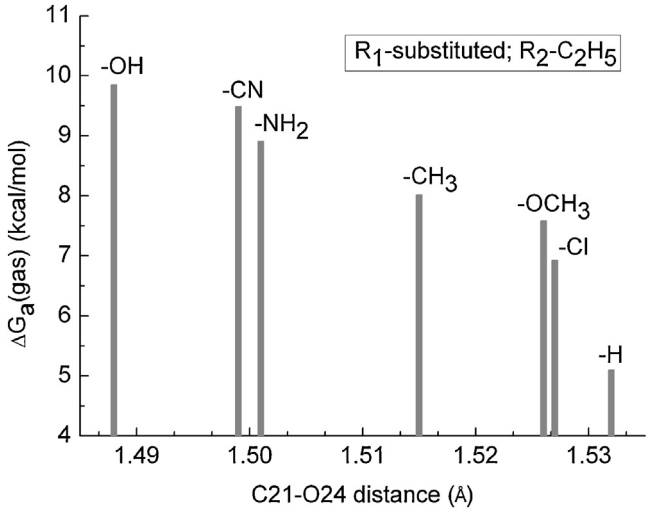

Fig. 7. Calculated ΔG_a^g related to C21—O24 distance of different intermediates with different substituents.

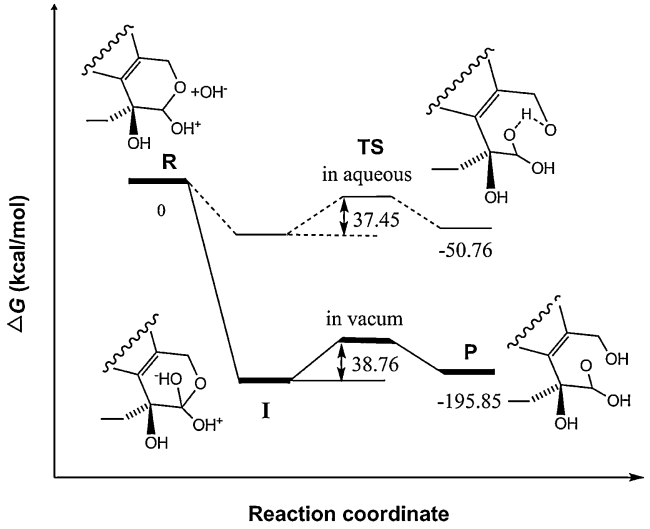

Fig. 8. Calculated reaction profiles of the CPT's E-ring-opening when O25 was protonated, solid lines: free energies in vacuo, dashed lines: free energies in aqueous phase. All the structural optimizations were carried out in CCl_4 and relative energies (in kcal/mol) were obtained at MP2/6−311+G(d,p)//B3LYP/6−31G(d,p) level of theory.

Table 3
Comparisons of the ΔG_a and the ΔG_r (in kcal/mol) of CPT, SN-38 and Topotecan in vacuo and in aqueous solution, respectively.

	ΔG_a^g	ΔG_a^a	ΔG_r^a
CPT	9.85	12.94	−31.84
SN-38	7.15	10.51	−33.49
Topotecan	9.64	12.86	−31.50

(All the structures of the substituent and the corresponding data of Fig. 6 are shown in Fig. S3 and Table S4, Supporting Information.)

3.2.2. A and B rings modifications

Up to now, the most successful hemi-synthetic derivatives of CPT are Topotecan and Irinotecan (CPT-11) [47,48], and they have already obtained the permission from American FDA of coming into market [49]. Since Irinotecan is a prodrug which needs to be converted to its active metabolite SN-38 [50], the typical CPT's derivatives Topotecan ((20S)-9-(dimethylamino)methyl-10-hydroxy-camptothecin) and SN-38 ((20S)-7-ethyl-10-hydroxy-camptothecin) (see Figs. 1 and S3) were therefore chosen to study the impact of modifying A and B rings on CPT's E-ring-opening reaction (see Table 3).

As listed in Table 3, the ΔG_a^g of SN-38 and Topotecan are 7.15 and 9.64 kcal/mol, and their ΔG_a^a are 10.51 and 12.86 kcal/mol, respectively. In contrast with that of CPT, 9.85 and 12.94 kcal/mol, both ΔG_a^g and ΔG_a^a are reduced by modifying A and B rings with substituents OH, CH_2—CH_3 and CH_2—$N(CH_3)_2$. Because the substituents are electron-donating groups, the presence of them would impact other rings more or less for the inductive effect. Compared with CPT, we would not attribute the high pharmic curative effects of SN-38 and Topotecan to the inhibition of E-ring-opening, but to the enhancement of the drug's lipophilic power, so the stability of E-ring increases in the human blood plasma.

So far the relationship between reactivity and different substituents on A, B and E rings has been completed. Though changes of structure would impact the reactivity, the process of CPT's E-ring opening did not be prevented. As mentioned in reference [27], Topotecan, when compared with its parental compound CPT, has increased solubility and pharmacological activity. Maybe the best method to advance the antitumor activity of CPT-basic drugs is not to restrain their E rings from opening, but to promote their solubility by introducing substituents.

3.3. Other Paths of CPT's E-ring-opening

We have also looked for other possible mechanisms of the E-ring-opening for CPT. In the first instance, we replaced the attacking hydroxyl by a water molecule, without any constraint of the molecule, the attacking water was found a large distance away from CPT. Even though the O25 was protonated, water did not attack C21 at all. By this token, water as a nucleophile is too weak to attack CPT's E-ring. Maybe this is the reason why CPT keeps lactone form if the PH value of buffer solution less than or equal to 5 [51]. In addition, we have also forced the reaction to proceed via the S_N2-type mechanism to compare with the addition coupled elimination mechanism. A transition state produced by QST2 method with giving reactants and products was found. However, it is a pity that the transition state is not the expected one that is accompanied by hydroxyl attacking and O24 leaving synchronously, but the same as that of elimination, so E-ring-opening reaction of CPT seems to be favored with the addition coupled elimination mechanism. Another potential path of E-ring-opening was found on the condition that O25 was protonated, and then C21 was attacked by a hydroxyl. However, the presence of the proton alters the elimination process absolutely. As shown in Fig. 8, the only transition state, characterized by an imaginary frequency of 1682 cm^{-1}, corresponds to the proton transfer, where the proton is vibrating between O43 and O24. The energy barrier of this process climbs remarkably with the value of 38.76 and 37.45 kcal/mol in vacuo and aqueous solution, respectively, and compared with the addition coupled elimination mechanism we proposed above, this path seems to be too tough for CPT to open its E-ring. (The corresponding structures of stationary point are shown in Fig. S4, Supporting Information.)

4. Conclusions

In the present work, the E-ring-opening mechanisms of CPT and its analogs have been revealed by using the quantum chemistry DFT method. The related geometries during the E-ring-opening processes were obtained at the B3LYP/6−31G(d,p) level in CCl_4, and the exact solvation free energies were calculated at the MP2/6−311+G(d,p) level by using the IEF-PCM model. The calculations show the following: (1) All the E-ring-opening reactions of CPT and its derivatives are spontaneous processes, conforming to

the addition coupled elimination pathway. This is consistent with the electrochemical reduction mechanism reported by Afzal Shaha et al. [19]. (2) In the aqueous solution, besides bonding to C21, the hydroxyl interacts with water molecules by forming hydrogen bonds, where the hydrogen acceptor is the oxygen of hydroxyl, and hydrogen donor is water. (3) The activation free energy increases as the number of participated explicit water molecules increases, and the corresponding ΔG_a^a is in agreement with the experimental value. (4) The effects of substituent on reactivity have also been discussed. The influencing factors of activation free energies include the electronic effect, the size of substituent, and the stability of intermediate. E-ring-opening mechanisms of CPT and its derivatives provided here are the basis of distinguishing the reactive direction and the activities of various substituent groups; it may be helpful to design drugs like CPT and to improve the anticancer activity of such drugs.

Acknowledgment

This research has been funded by the key grant from the National Natural Science Foundation of China (No. 21133005).

Appendix A. Supplementary data

Supplementary data associated with this article can be found, in the online version, at http://dx.doi.org/10.1016/j.jmgm.2013.03.004.

References

[1] M.E. Wall, M.C. Wani, C.E. Cooke, K.H. Palmer, A.T. McPhail, G.A. Slim, Plant antitumor agents. I. The isolation and structure of camptothecin, a novel alkaloidal leukemia and tumor inhibitor from *Camptotheca acuminata*, Journal of the American Chemical Society 88 (1966) 3888–3890.
[2] M.E. Wall, M.C. Wani, Camptothecin and taxol discovery to clinic—thirteenth Bruce F. Cain memorial award lecture, Cancer Research 55 (1995) 753–760.
[3] C. Zazza, A. Coletta, N. Sanna, G. Chillemi, G. Mancini, A. Desideri, Solvent effects on the valence UV–vis absorption spectra of Topotecan anticancer drug in aqueous solution at room temperature: a nanoseconds time-scale TD-DFT/MD computational study, Journal of Physical Chemistry B 114 (2010) 6770–6778.
[4] M.E. Wall, Camptothecin and taxol discovery to clinic, Medicinal Research Reviews 18 (1998) 299–314.
[5] Y.H. Hsiang, R. Hertzberg, S. Hecht, L.F. Liu, Camptothecin induces protein-linked DNA breaks via mammalian DNA topoisomerase I, Journal of Biological Chemistry 260 (1985) 14873–14878.
[6] Y.H. Hsiang, L.F. Liu, Identification of mammalian DNA topoisomerase I as an intracellular target of the anticancer drug camptothecin, Cancer Research 48 (1988) 1722–1726.
[7] R.N. Jena, P.C. Mishra, A theoretical study of some new analogues of the anticancer drug camptothecin, Journal of Molecular Modeling 13 (2007) 267–274.
[8] M. Gupta, A. Fujimori, Y. Pommier, Eukaryotic DNA topoisomerases I, Biochimica et Biophysica Acta 1262 (1995) 1–14.
[9] J. Wu, L.F. Liu, Processing of topoisomerase I cleavable complexes into DNA damage by transcription, Nucleic Acids Research 25 (1997) 4181–4186.
[10] Y. Pommier, DNA topoisomerase I inhibitors: chemistry, biology, and interfacial inhibition, Chemical Reviews 109 (2009) 2894–2902.
[11] Z. Mi, T.G. Burke, Differential interactions of camptothecin lactone and carboxylate forms with human blood components, Biochemistry 33 (1994) 10325–10336.
[12] L.J. Zhu, C.L. Zhuang, N. Lei, Z.Z. Guo, C.Q. Sheng, G.Q. Dong, S.Z. Wang, Y.Q. Zhang, J.Z. Yao, Z.Y. Miao, W.N. Zhang, Synthesis and preliminary bioevaluation of novel E-ring modified acetal analog of camptothecin as cytotoxic agents, European Journal of Medical Chemistry 56 (2012) 1–9.
[13] T.G. Burke, Z.M. Mi, The structural basis of camptothecin interactions with human serum albumin: impact on drug stability, Journal of Medicinal Chemistry 37 (1994) 40–46.
[14] S.M. Hecht, Camptothecin: roles of the D and E rings in binding to the topoisomerase I-DNA covalent binary complex, Current Medicinal Chemistry: Anti-Cancer Agents 5 (2005) 353–362.
[15] X.S. Xiao, M. Cushman, Effect of E-ring modifications in camptothecin on topoisomerase I. inhibition: a quantum mechanics treatment, Journal of Organic Chemistry 70 (2005) 9584–9587.
[16] D. Dvoranová, V. Brezová, M. Valko, A. Stasko, Photoinduced transformation of camptothecin in the presence of iron(III) ions, Journal of Photochemistry and Photobiology A: Chemistry 185 (2007) 172–180.
[17] M. Li, W. Tang, F. Zeng, L. Lou, T. You, Semi-synthesis and biological activity of c-lactones analogs of camptothecin, Bioorganic and Medicinal Chemistry Letters 18 (2008) 6441–6443.
[18] R.P. Hertzberg, M.J. Caranfa, K.G. Holden, D.R. Jakas, G. Gallagher, M.R. Mattern, S.M. Mong, J.O. Bartus, R.K. Johnson, W.D. Kingsbury, Modification of the hydroxy lactone ring of camptothecin: inhibition of mammalian topoisomerase I and biological activity, Journal of Medicinal Chemistry 32 (1989) 715–720.
[19] B. Afzal Shaha, V.C. Diculescua, R. Qureshib, M. Oliveira-Bretta, Electrochemical reduction mechanism of camptothecin at glassy carbon electrode, Bioelectrochemistry 79 (2010) 173–178.
[20] J. Dey, I.M. Warner, Excited state tautomerization of camptothecin in aqueous solution, Journal of Photochemistry and Photobiology A: Chemistry 101 (1996) 21–27.
[21] J. Dey, I.M. Warner, Spectroscopic and photophysical studies of the anticancer drug: camptothecin, Journal of Luminescence 71 (1997) 105–114.
[22] Y. Posokhov, H. Biner, S. Icli, Spectral-luminescent and solvatochromic properties of anticancer drug camptothecin, Journal of Photochemistry and Photobiology A: Chemistry 158 (2003) 13–20.
[23] H. Zhao, C. Lee, P. Sai, Y.H. Choe, M. Boro, A. Pendri, S. Guan, R.B. Greenwald, 20-O-acylcamptothecin derivatives: evidence for lactone stabilization, Journal of Organic Chemistry 65 (2000) 4601–4606.
[24] S.A. Strel'tsov, S.L. Grokhovskii, I.A. Kudelina, V.A. Oleinikov, A.L. Zhuze, Interaction of Topotecan, DNA topoisomerase I inhibitor, with double-stranded polydeoxyribonucleotides. 1. Topotecan dimerization in solution, Molecular Biology 35 (2001) 432–441.
[25] K.M. Solntsev, E.N. Sullivan, L.M. Tolbert, S. Ashkenazi, P. Leiderman, D. Huppert, Excited-state proton transfer reactions of 10-hydroxycamptothecin, Journal of the American Chemical Society 126 (2004) 12701–12708.
[26] S. Kunadharaju, M. Savva, Kinetic and thermodynamic analysis of 10-hydroxy-camptothecin hydrolysis at physiological pH, Journal of Chemical Thermodynamics 40 (2008) 1439–1444.
[27] N. Sanna, G. Chillemi, A. Grandi, S. Castelli, A. Desideri, V. Barone, New hints on the pH-driven tautomeric equilibria of the Topotecan anticancer drug in aqueous solutions from an integrated spectroscopic and quantum-mechanical approach, Journal of the American Chemical Society 127 (2005) 15429–15436.
[28] C. Lee, W. Yang, R.G. Parr, Development of the Colle-Salvetti correlation-energy formula into a functional of the electron density, Physical Review B 37 (1988) 785–789.
[29] C. Moller, M.S. Plesset, Note on an approximation treatment for many-electron systems, Physical Review 46 (1934) 618–622.
[30] M.J. Frisch, et al., Gaussian 03, Gaussian Inc., Pittsburgh, PA, 2003.
[31] C. Gonzalez, H.B. Schlegel, An improved algorithm for reaction path following, Journal of Chemical Physics 90 (1989) 2154–2161.
[32] C. Gonzalez, H.B. Schlegel, Reaction path following in mass-weighted internal coordinates, Journal of Physical Chemistry 94 (1990) 5523–5527.
[33] B. Mennucci, J. Tomasi, Continuum solvation models: a new approach to the problem of solute's charge distribution and cavity boundaries, Journal of Chemical Physics 106 (1997) 5151–5158.
[34] B. Mennucci, E. Cances, J. Tomasi, Evaluation of solvent effects in isotropic and anisotropic dielectrics and in ionic solutions with a unified integral equation method: theoretical bases, computational implementation, and numerical applications, Journal of Physical Chemistry B 101 (1997) 10506–10517.
[35] J. Tomasi, B. Mennucci, E. Cances, The IEF version of the PCM solvation method: an overview of a new method addressed to study molecular solutes at the QM ab initio level, Journal of Molecular Structure: THEOCHEM 464 (1999) 211–226.
[36] C.S. Wang, Z.Z. Yang, Atom-bond electronegativity equalization method. II. Lone-pair electron model, Journal of Chemical Physics 110 (1999) 6189–6197.
[37] Y. Cong, Z.Z. Yang, General atom-bond electronegativity equalization method and its application in prediction of charge distributions in polypeptide, Chemical Physics Letters 316 (2000) 324–329.
[38] D.X. Zhao, C. Liu, F.F. Wang, C.Y. Yu, L.D. Gong, S.B. Liu, Z.Z. Yang, Development of a polarizable force field using multiple fluctuating charges per atom, Journal of Chemical Theory and Computation 6 (2010) 795–804.
[39] D. Asthagiri, L.R. Pratt, J.D. Kress, M.A. Gomez, Hydration and mobility of HO(aq), Proceedings of the National Academy of Sciences of the United States of America 101 (2004) 7229–7233.
[40] S.S. Xantheas, Theoretical study of hydroxide ion-water clusters, Journal of the American Chemical Society 117 (1995) 10373–10380.
[41] M. Miechowski, J. Stangret, Hydroxide ion hydration in aqueous solutions, Journal of Physical Chemistry A 111 (2007) 2889–2897.
[42] A. Warshel, M. Levitt, Theoretical studies of enzymic reactions: dielectric, electrostatic and steric stabilization of the carbonium ion in the reaction of lysozyme, Journal of Molecular Biology 103 (1976) 227–249.
[43] U.C. Singh, P.A. Kollman, A combined *ab initio* quantum mechanical and molecular mechanical method for carrying out simulations on complex molecular systems: applications to the CH3Cl + Cl^- exchange reaction and gas phase protonation of polyethers, Journal of Computational Chemistry 7 (1986) 718–730.
[44] M.J. Field, P.A. Bash, M. Karplus, A combined quantum mechanical and molecular mechanical potential for molecular dynamics simulations, Journal of Computational Chemistry 11 (1990) 700–733.
[45] M.E. Wall, M.C. Wani, A.W. Nicholas, G. Manikumar, C. Tele, L. Moore, A. Truesdale, P. Leitner, J.M. Besterman, Plant antitumor agents. 30. Synthesis and structure activity of novel camptothecin analogs, Journal of Medicinal Chemistry 36 (1993) 2689–2700.

[46] C. Jaxel, K.W. Kohn, M.C. Wani, M.E. Wall, Y. Pommier, Structure–activity study of the actions of camptothecin derivatives on mammalian topoisomerase I: evidence for a specific receptor site and a relation to antitumor activity, Cancer Research 49 (1989) 1465–1469.
[47] A. Tanizawa, A. Fujimori, Y. Fujimori, Y. Pommier, Comparison of topoisomerase I inhibition, DNA damage, and cytotoxicity of camptothecin derivatives presently in clinical trials, Journal of the National Cancer Institute 86 (1994) 836–842.
[48] A. Tanizawa, K.W. Kohn, G. Kohlhagen, F. Leteurtre, Y. Pommier, Differential stabilization of eukaryotic DNA topoisomerase I cleavable complexes by camptothecin derivatives, Biochemistry 34 (1995) 7200–7206.
[49] Y. Pommier, P. Pourquier, Y. Urasaki, J. Wu, G.S. Laco, Topoisomerase I inhibitors: selectivity and cellular resistance, Drug Resistance Updates 2 (1999) 307–318.
[50] Y. Kawato, M. Aonuma, Y. Hirota, H. Kuga, K. Sato, Intracellular roles of SN-38, a metabolite of the camptothecin derivative CPT-11, in the antitumor effect of CPT-11, Cancer Research 51 (1991) 4187–4191.
[51] N. Sanna, G. Chillem, L. Gontrani, A. Grandi, G. Mancini, S. Castelli, G. Zagotto, C. Zazza, V. Barone, A. Desideri, UV–vis spectra of the anticancer campothecin family drugs in aqueous solution: specific spectroscopic signatures unraveled by a combined computational and experimental study, Journal of Physical Chemistry B 113 (2009) 5369–5375.